



Original Research Article

A comprehensive DFT study on the adsorption of tetryl on the surface of graphene

Mohammad Reza Jalali Sarvestani^a, Roya Ahmadi^{b,*}

^a Young Researchers and Elite Club, Yadegar-e-Imam Khomeini (RAH) Shahr-e-Rey Branch, Islamic Azad University, Tehran, Iran

^b Department of Chemistry, Yadegar-e-Imam Khomeini (RAH) Shahr-e-Rey Branch, Islamic Azad University, Tehran, Iran

ARTICLE INFORMATION

Received: 19 March 2019
Received in revised: 11 May 2019
Accepted: 15 May 2019
Available online: 18 September

DOI: 10.22034/AJGC/2020.3.4

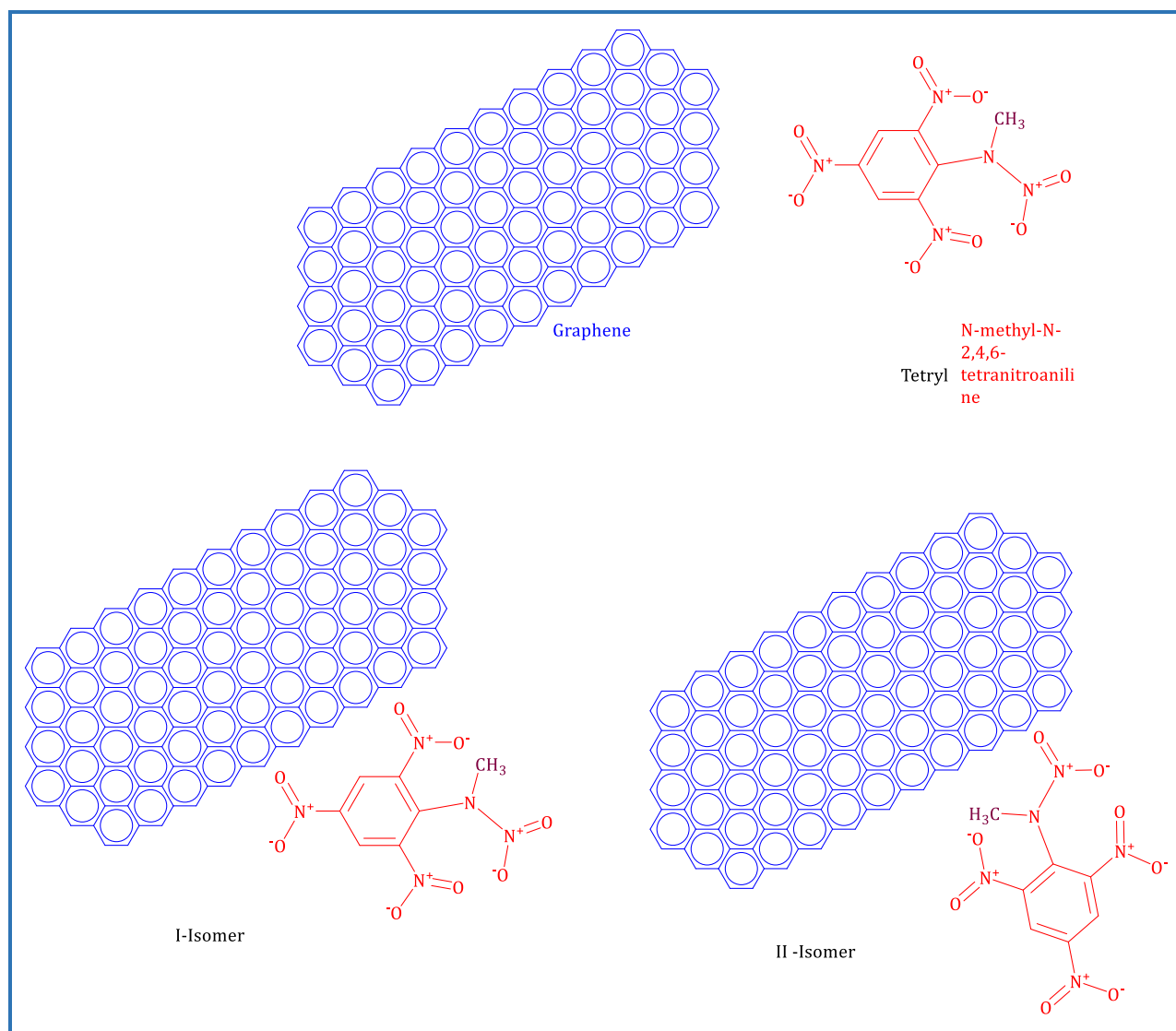
KEYWORDS

Tetryl
Graphene
Density functional theory
Explosive materials
Heat sensitivity

ABSTRACT

In this research study, computational simulation was used to study the adsorption of tetryl on the surface of graphene. For this purpose, the structures of graphene, tetryl and their complexes were optimized geometrically. Then, IR and Frontier molecular orbital calculations were implemented at 298-398 K at the intervals of 10°. The obtained thermodynamic parameters including, Gibbs free energy (ΔG_{ad}), adsorption enthalpy alterations (ΔH_{ad}), and thermodynamic equilibrium constants (K_{th}) revealed the adsorption of tetryl is exothermic, spontaneous, non-equilibrium, and experimentally feasible at the both evaluated configurations. The influence of temperature on the thermodynamic factors of the desired process was also evaluated and the results indicated that the 298.15 K was the best temperature for the graphene interaction with tetryl. The calculated specific heat capacity (CV) values revealed that the sensitivity of the produced graphene-tetryl complexes to the heat and shock have declined significantly. The increased nitrogen-oxygen bond lengths after the adsorption of tetryl to the surface of graphene exhibited that the explosive and destructive power of tetryl-graphene derivatives was higher than that of the pure tetryl. Some HOMO-LUMO related parameters such as energy gap, electrophilicity, chemical hardness, maximum transferred charge index (ΔN_{max}), and chemical potential were also calculated and discussed in details. © 2020 by SPC (Sami Publishing Company), Asian Journal of Green Chemistry, Reproduction is permitted for noncommercial purposes.

Graphical Abstract

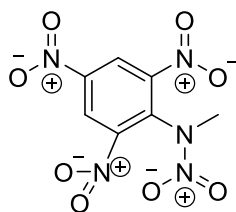


Introduction

The matter of finding new explosives material with great blasting power and low sensitivity to heat, shock and friction has been very controversial in recent decades [1, 2]. However, one of the mains challenges in front of chemists, which discouraged research and development activities on explosive materials, is that this category of substances is very dangerous and toxic and can endanger the scholar's health and safety [3–5]. Moreover, in many cases, chemists synthesized new compounds with high costs but unfortunately, the synthesized substances did not have appropriate features of an ideal explosive [6–8]. In other words, in spite of the huge budgets that had been allocated to those studies, the results of the implemented surveys were counterproductive [9–11]. On the other hand, computational methods can provide opportunity for the scientists to investigate the field of energetic

material without taking risks and endangering their lives [12–16]. In addition, the properties of new compounds can also be predicted by theoretical studies in advance with low cost. Therefore, carrying out computational investigations before experimental studies can be so beneficial [17–19].

Tetryl (As shown in Scheme 1) is a blasting substance that has been widely used in the construction of bombs and war ammunition in the first and second world wars [20]. The IUPAC name of tetryl is *N*-methyl-*N*-2,4,6-trinitroaniline with yellow color [21–23]. This compound was first described by Romburgh at 1883 and for its synthesis dimethylaniline should be dissolved in concentrated sulfuric acid at the outset to form dimethylaniline sulfate. In the next step, a mixture of H_2SO_4 and HNO_3 should be utilized for the nitration reaction and producing tetryl. Tetryl is a well-known energetic compound due to its unique features so that it was recognized as one of the most efficient blasting material during the first world war. Moreover, explosion velocity of tetryl is about 7200 to 7300 m/s and its power and sensitivity is more than trinitrotoluene (TNT) [24–26]. One of the main disadvantages of explosives is their sensitivity to heat, shock and friction. This is due to the fact that, if an energetic compound has a high sensitivity to these factors it might explode in an inappropriate circumstance and creates irreparable damages. In this regards, finding novels explosive materials with a high blasting potent and low sensitivity to heat, shock and friction, is very crucial [27]. Moreover, graphene is a two-dimensional nanostructure material that is entailed of carbon atoms, which are connected to each other by sp^2 hybrid, and it is consisting of resembling hexagonal rings like the benzene (Figure 1). Graphene was introduced for the first time in 1986 and the graphene name is originated from the combination of graphite word and suffix (ene) which refers to multi-ring aromatic hydrocarbons. As graphene is a porous carbon substance with an outstanding specific surface area and unique structure, it has prominent chemical, physical, and energetic traits. Therefore, the impressions of graphene on the structural and energetic properties of tetryl were assessed using density functional theory (DFT) for the first time, in this research [28–32].



***N*-methyl-*N*-(2,4,6-trinitrophenyl)nitramide**

Scheme 1. The chemical structure and IUPAC name of tetryl

Experimental

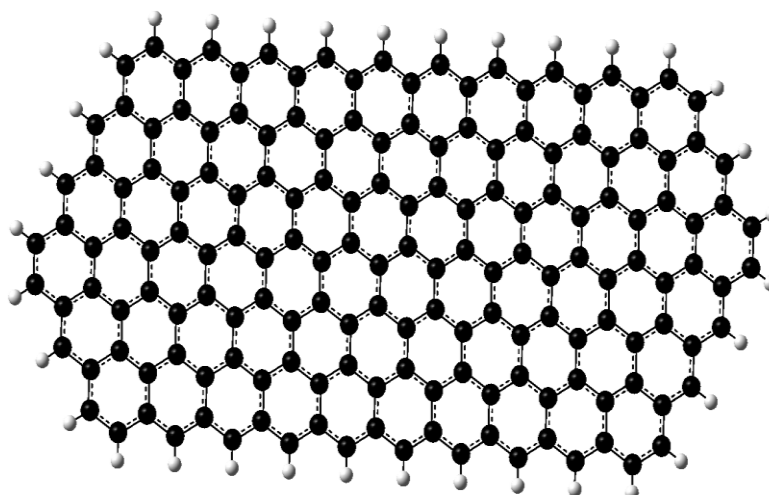


Figure 1. The structure of single-layer graphene

Computational details

At the outset, the structures of graphene, tetryl and their derived products at two nanotube modeller 1.3.0.3 and Gauss view softwares designed various configurations. Afterward, the designed structures were optimized geometrically. In the next step, IR and Frontier molecular orbital calculations were implemented at 298-398 K at 10° intervals using the Spartan software. The computations performed in the atmospheric pressure and aqueous phase. The DFT method and B3LYP/631G (d) basis set were chosen for the calculations because, in former studies, this method and basis set had produced results that were in an admissible accordance with the experimental findings [33]. The evaluated process was as follows:



Results and Discussion

Evaluating structural features

As it is clear from [Figure 2a](#), the interaction of tetryl and graphene was investigated at two configurations. The derived product that is originated from the insertion of 6th carbon atom of tetryl near to the surface of graphene is remarked by I-Isomer name ([Figure 2b](#)). In addition, the II-Isomer abbreviated name was considered for the derivative that is produced from the placing of 7th carbon atom of tetryl on the surface of graphene nanostructure ([Figure 2c](#)).

The nitrogen-oxygen bond lengths are a key factor that can affect the destructive and blasting power of energetic compounds with nitro functional groups in their structures. In this regards, when

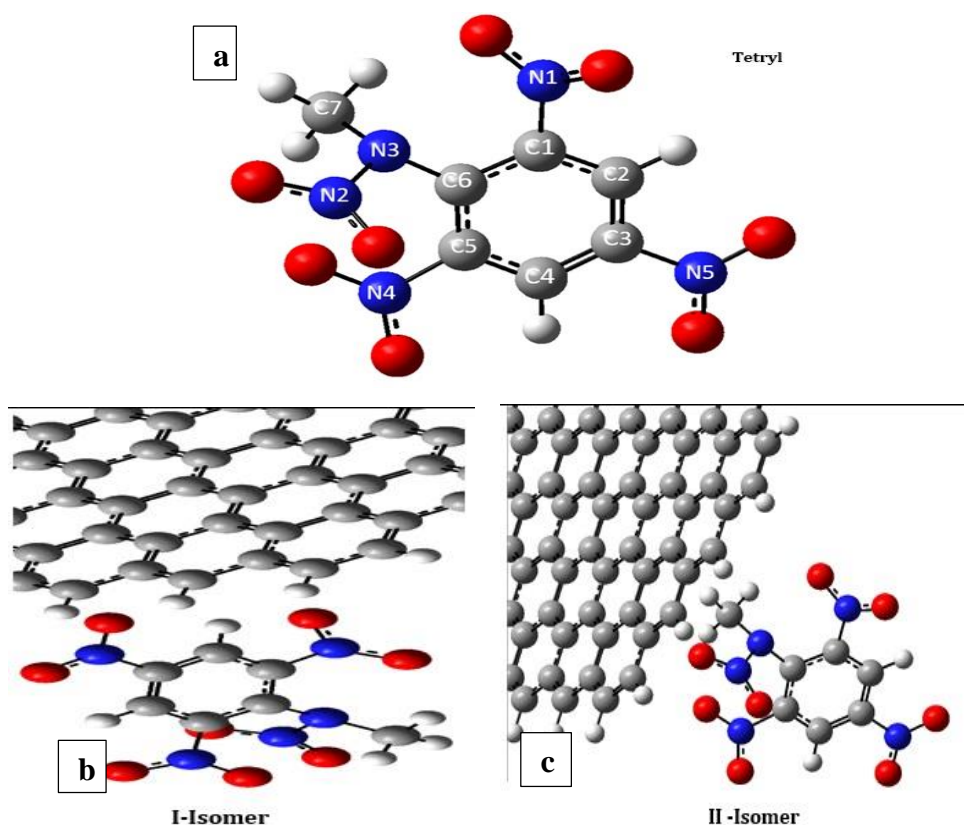


Figure 2. The optimized structures of tetryl and its complexes with graphene at two various configurations

the software designed the desired structures, geometrical optimizations were performed on them and the N-O bond lengths were presented in Table 1. As it can be perceived from Table 1, after the adsorption of tetryl on the surface of graphene nano sheet, the N-O bond lengths have incremented substantially. The increased nitrogen-oxygen bond lengths in tetryl-graphene derivatives proved that the bonds between nitrogen and oxygen have become weaker. In addition, the explosive material can undergo combustion and explosion reactions more conveniently. Therefore, the derived products from the interaction of graphene with tetryl are stronger explosives than the pure tetryl. By comparing the bond lengths of I-Isomer with II-Isomer, it will be realized that they do not have a meaningful discrepancy in their N-O bond lengths. Therefore, it seems the explosive power of both isomers should be very close to each other. The next matter that can be witnessed from the Table 1 is that the total energy values of both graphene-tetryl derivatives are more negative than pure tetryl. In fact, I-Isomer and II-Isomer are more stable and less reactive compared with the single tetryl in energetic aspects. It should be noted that because of the carried out IR computations, it was not seen any negative frequency at all of the studied structures.

Calculation and verifying the values of adsorption enthalpy changes (ΔH_{ad})

Table 1. Total energy, lowest frequency and bond lengths of tetryl and its derived products with graphene

	Tetryl	I-Isomer	II -Isomer
Total energy (a.u)	-1123.575	-2319.915	-2320.042
Lowest frequency (cm ⁻¹)	31.169	10.324	10.237
N ₁ -O ₁ (Å)	1.27863	1.3762	1.38467
N ₁ -O ₂ (Å)	1.27534	1.36527	1.43784
N ₂ -O ₁ (Å)	1.26808	1.38608	1.38721
N ₂ -O ₂ (Å)	1.2764	1.4247	1.44899
N ₄ -O ₁ (Å)	1.27782	1.43237	1.39432
N ₄ -O ₂ (Å)	1.27635	1.49088	1.39172
N ₅ -O ₁ (Å)	1.27745	1.3514	1.35342
N ₅ -O ₂ (Å)	1.27842	1.36634	1.36797
C ₆ -C (Å)	---	1.50726	---
C ₇ -C (Å)	---	---	1.53123

The Equation 2 was used to acquire the enthalpy variations for the adsorption process of tetryl. In this formula, H represents the sum of the thermal correction of enthalpy with the total energy for the reactants and products of the evaluated process [33-36].

$$\Delta H_{ad} = H_{(Tetryl-Ger)} - (H_{(Tetryl)} + H_{(Ger)}) \quad (2)$$

The provided data in Table 2 indicates that interaction of the tetryl with graphene is exothermic at both configurations as the achieved ΔH_{ad} values are negative for both isomers. The influence of temperature on this variable was also evaluated. As seen in Table 2, temperature does not have an obvious effect on enthalpy changes. This is due to the fact that, there is not a remarkable difference between the obtained ΔH_{ad} values at different temperatures. Therefore, 298 K can be selected as the best temperature for the adsorption procedure of tetryl. The next hidden point in the Table 2 is that II-Isomer has lower enthalpy changes in comparison to I-Isomer at all temperatures. Thus, it can be deduced that the formation of II-Isomer is more exothermic and experimentally possible than the formation process of I-Isomer.

Calculation and inquiring the values of Gibbs free energy alterations (ΔG_{ad}) and thermodynamic equilibrium constants (K_{th})

Table 2. The values of enthalpy changes for the adsorption of tetryl on the surface of graphene in the temperature range of 298-398 K

Temperature (K)	ΔH_{ad} (KJ/mol)	
	I-Isomer	II-Isomer
298	-1396.651	-1724.377
308	-1396.577	-1724.351
318	-1396.546	-1724.318
328	-1396.528	-1724.311
338	-1396.515	-1724.296
348	-1396.504	-1724.261
358	-1396.485	-1724.256
368	-1396.476	-1724.267
378	-1396.478	-1724.282
388	-1396.518	-1724.349
398	-1396.504	-1724.415

Equation 3 was used to calculate the Gibbs free energy changes. In this equation, G stands for the sum of the thermal correction of Gibbs free energy and the total energy that was computed by the software for the reactants and products of the desired procedure [33–36].

$$\Delta G_{ad} = G_{(Tetryl-Ger)} - (G_{(Tetryl)} + G_{(Ger)}) \quad (3)$$

The values of Gibbs free energy changes for the adsorption of tetryl on the surface of graphene in the temperature range of 298-398 K are reported in Table 3. As demonstrated in Table 3, the adsorption of tetryl at both configurations are spontaneous due to the remarkable negative calculated Gibbs free energy changes. The impression of temperature on this variable was also assessed. The results showed that, by enhancing the temperature, ΔG_{ad} was reduced gradually. It was found that, the ambient temperature was the best for the adsorption process of tetryl. Moreover, the values of Gibbs free energy changes for II-Isomer was lower than I-Isomer. Therefore, the formation process of the II-Isomer is more spontaneous and experimentally feasible than the other product.

The thermodynamic equilibrium constants of the desired procedure were also calculated using Equation 4. In this formula, T denotes the temperature, R is the ideal gas constant and ΔG_{ad} is the obtained values of Gibbs free energy changes that were calculated in the last section [33–36].

$$K_{th} = \exp (-\Delta G_{ad} / RT) \quad (4)$$

As seen in Table 4, the formation I-Isomer and II-Isomer is one-sided and non-equilibrium. One of the main upsides of the thermodynamic constant is that it can show the effect of temperature more sharply than the other parameters. As seen in Table 4, by increasing the temperature, thermodynamic equilibrium constant values variable has declined significantly. Therefore, 298.15 K is the optimum temperature for the interaction of tetryl with graphene. In addition, K_{th} values of II-Isomer is more positive than I-Isomer. Therefore, it can be elicited that, formation of the II-Isomer is more one-sided and non-equilibrium than the other Isomer.

Table 3. The values of Gibbs free energy changes for the adsorption of tetryl on the surface of graphene in the temperature range of 298-398 K

Temperature (K)	ΔG_{ad} (KJ/mol)	
	I-Isomer	II-Isomer
298	-1328.829	-1650.713
308	-1326.468	-1648.131
318	-1324.075	-1645.547
328	-1321.697	-1642.993
338	-1319.286	-1640.425
348	-1316.836	-1637.775
358	-1314.414	-1635.247
368	-1311.964	-1632.728
378	-1309.462	-1630.218
388	-1306.902	-1627.724
398	-1304.292	-1625.1951

Table 4. Thermodynamic equilibrium constant values for the adsorption of tetryl on the surface of graphene in the temperature range of 298-398 K

Temperature (K)	K_{th}	
	I-Isomer	II-Isomer
298	$6.512 \times 10^{+232}$	$1.616 \times 10^{+289}$
308	$7.215 \times 10^{+224}$	$2.430 \times 10^{+279}$
318	$2.499 \times 10^{+217}$	$1.513 \times 10^{+270}$
328	$2.479 \times 10^{+210}$	$3.465 \times 10^{+261}$
338	$6.308 \times 10^{+203}$	$2.562 \times 10^{+253}$
348	$3.789 \times 10^{+197}$	$5.398 \times 10^{+245}$
358	$5.111 \times 10^{+191}$	$3.179 \times 10^{+238}$

368	$1.424 \times 10^{+186}$	$4.640 \times 10^{+231}$
378	$7.677 \times 10^{+180}$	$1.561 \times 10^{+225}$
388	$7.595 \times 10^{+175}$	$1.138 \times 10^{+219}$
398	$1.320 \times 10^{+171}$	$1.669 \times 10^{+213}$

Calculation and examining the values of specific heat capacity (C_V)

Because the specific heat capacity has a direct relationship with the sensitivity to heat and shock, its determination is very important. Specific heat capacity is described as the amount of heat and energy, which is needed for increasing the temperature of a certain amount of a substance to 1 degree. Indeed, when a compound has a higher value of C_V , it will be less sensitive to heat and shock because it demands more heat to raise its temperature whereas a compound with a low value of C_V will be more sensitive to heat and shock. For this reason, this parameter was also calculated and presented in Table 5. As it can be seen from Table 5, the specific heat values of graphene-tetryl derivatives are higher than pure tetryl. In other words, graphene-tetryl derived products are less sensitive to heat and shock because they require more heat to enhance their temperature to one degree. By a more precise look at the table, it will be realized that the C_V values of I-isomer are more positive than II-Isomer. Therefore, it could be inferred that I-Isomer is safer than the other derivative. The impact of temperature on this parameter was also inspected. As it is clear by raising the temperature, the specific heat capacity of pure tetryl and graphene-tetryl derivatives has also increased linearly.

Frontier molecular orbital analysis

Some of the chemical and structural traits of tetryl and its complexes with graphene including the energy of HOMO and LUMO orbitals (E_H and E_L), the energy discrepancy between HOMO and LUMO molecular orbitals (HLG), the electrophilicity index (ω), maximum transferred charge index (ΔN_{\max}), chemical potential (μ), zero-point energy, density, chemical hardness (η), dipole moment, volume and weight were calculated and reported in Table 6. In chemistry, HOMO is the highest occupied molecular orbital, LUMO is the lowest unoccupied molecular orbital, and the energy difference between them is described as an energy gap, which is usually represented by HLG symbol. It should be mentioned that HLG variable was calculated by using Equation 5. The provided data in Table 6 demonstrates that the energy gap has increased after the adsorption of tetryl on the graphene nano sheet. In addition, this rising is more significant in the case of II-Isomer. Energy gap has a direct relationship with conductivity so that the compounds with low HLG are more conductive than

compounds with high HLG values because a high amount of HLG implies that the substance needs more energy for transferring the electron to the excited state. Hence, it can be deduced that the conductivity of pure tetryl is more than its derivatives with graphene owing to the incrementing trend of HLG.

Table 5. The specific heat capacity values of tetryl and its derivatives with graphene in the temperature range of 298-398 K

Temperature (K)	Cv (J/mol.K)		
	Tetryl	I-Isomer	II-Isomer
298	252.953	594.839	579.674
308	258.555	610.276	595.404
318	264.086	625.447	610.88
328	269.548	640.356	626.103
338	274.938	655.006	641.072
348	280.258	669.399	655.789
358	285.507	683.536	670.252
368	290.683	697.419	684.461
378	295.787	711.046	698.414
388	300.816	724.42	712.112
398	305.771	737.539	725.552

Table 6. The values of calculated E_H and E_L , HLG, chemical hardness (η), electrophilicity index (ω), the chemical potential (μ), the maximum amount of electronic charge index (ΔN_{max}), volume, weight, density, zero point energy and dipole moment

	Chemical properties		
	Tetryl	I-Isomer	II-Isomer
E_H (eV)	-8.22	-6.91	-7.87
E_L (eV)	2.68	6.41	6.35
HLG (eV)	10.9	13.32	14.22
η (eV)	5.45	6.66	7.11
μ (eV)	-2.77	-0.25	-0.76
ω (eV)	0.7	0	0.04
ΔN_{max} (eV)	0.51	0.04	0.11
Dipole moment (deby)	3.17	4.64	2.34
Volume (\AA^3)	220.21	598.47	598.05
Weight (amu)	287.14	670.49	670.49

Area (Å ²)	249.13	555.6	548.96
Density=m/v (amu/Å ³)	1.3	1.12	1.12
Zero point energy (KJ/mol)	444.08	873.81	884.89

Chemical hardness was the next studied parameter, which was calculated using Equation 6. In addition, this parameter is related to the reactivity of the structure. Due to the fact that, the soft compounds can alter their electron density more conveniently in comparison with hard substances. Therefore, soft molecules can participate in chemical reactions more easily because the electron transmission, which is necessary for the implementation of reactions, can be done better in this type of compounds. As can be seen, in Table 6, chemical hardness has incremented after the adsorption of tetryl on the surface of graphene. Therefore, tetryl-graphene derivatives are more chemically harder and less reactive than pure tetryl. The amount of chemical potential, which is essential for obtaining electrophilicity and maximum transferred charge capacity, was also calculated by Equation 7. Chemical potential experienced a tangible surge by binding of tetryl to the surface of graphene [33–36].

$$HLG = E_{LUMO} - E_{HOMO} \quad (5)$$

$$\eta = (E_{LUMO} - E_{HOMO})/2 \quad (6)$$

$$\mu = (E_{LUMO} + E_{HOMO})/2 \quad (7)$$

$$\omega = \mu^2/2\eta \quad (8)$$

$$\Delta N_{max} = -\mu/\eta \quad (9)$$

The electrophilicity index is an admissible criterion for checking out the tendency of a compound for absorbing the electron. This parameter was calculated using Equation 8. When two molecules react with each other, one of them play the role of a nucleophile whilst the other one acts as an electrophile. A material with high electrophilicity value will have a higher tendency to absorb electron. The maximum transmitted charge capacity (ΔN_{max}) can be calculated using Equation 9. A compound with a positive amount of ΔN_{max} will act as an electron acceptor and a material with a negative amount of ΔN_{max} will behave as an electron donor. As it can be witnessed, the amount of the both mentioned parameters have declined in tetryl-graphene derived products, which substantiates that pure tetryl has a higher propensity towards electron in comparison to its derivatives with graphene. The next evaluated parameter is dipole moment, which has an obvious relationship with

the solubility of the studied compound in polar solvents like water. The dipole moment of I-Isomer is higher than the dipole moment of pure tetryl and II-Isomer. Therefore, I-Isomer has better solubility in polar solvents whereas the solubility of pure tetryl and II-Isomer is relatively poor in comparison to I-Isomer. The density values of the structure were also checked out. As it is obvious from Table 6, the density of tetryl has decreased after its reaction with graphene. Density has a direct relationship with explosion velocity, water resistance and detonation pressure. An energetic substance with a great density will have higher detonation velocity, pressure, and better water resistance. Therefore, the derived products from the reaction of tetryl with graphene have lower explosion velocity, detonation pressure and water resistance in comparison to pure tetryl.

Conclusions

Synthesis of new explosive materials with higher blasting power and lower sensitivity to heat, shock and friction is very important. In addition, theoretical methods help scientists to focus on this field without endangering their lives. In this regards, graphene doping effects on the energetic properties of tetryl were investigated in this study. The results indicated that the reaction of tetryl and graphene was exothermic, spontaneous, one-sided and experimentally possible and 298.15 K was the best temperature for the implementation of this reaction. Moreover, the sensitivity of tetryl to heat and shock has reduced after its adsorption on the graphene nano sheet. The N-O bond lengths have shown that the explosion power of tetryl-graphene derived products can be higher than pure tetryl. As the theoretical results proved, the tetryl adsorption on the surface of graphene can eventuate to explosives with lower shock and heat sensitivity and higher safety. The experimental investigation of this adsorption process is also recommended.

Acknowledgements

The author appreciates the Islamic Azad University of Yadegar-e-Imam Khomeini (RAH), Shahre-rey branch Research Council for the support of this project.

Disclosure Statement

No potential conflict of interest was reported by the authors.

References

- [1]. Ayoub K., Van Hullebusch E.D., Cassir M., Bermond A. *J. Hazard. Mater.*, 2010, **178**:10
- [2]. Panz K., Miksch K. *J. Environ. Manage.*, 2012, **113**:85

- [3]. Zhang J.G., Niu X.Q., Zhang S.W., Zhang T.L., Huang H.S., Zhou Z.N. *Comput. Theor. Chem.*, 2011, **964**:291
- [4]. Wu J.T., Zhang J.G., Yin X., He P., Zhang T.L. *Eur. J. Inorg. Chem.*, 2014, **27**:4690
- [5]. Zhao Z., Du Z., Han Z., Zhang Y., He C. *J. Energ. Mater.*, 2016, **34**:183
- [6]. Lin Q.H., Li Y.C., Qi C., Liu W., Wanga Y., Pang S.P. *J. Mater.Chem. A*, 2013, **1**:6776
- [7]. Joo Y.H., Shreeve J.M. *Angew. Chem. Int. Ed.*, 2010, **49**:7320
- [8]. Zhang J., Shreeve J.M. *J. Am. Chem. Soc.*, 2014, **136**:4437
- [9]. Talawar M.B., Sivabalan R., Mukundan T., Muthurajan H., Sikder A.K., Gandhe B.R., Subhananda Rao A. *J. Hazard. Mater.*, 2009, **161**:589
- [10]. Bahrami Panah N., Vaziri R. *Int. J. Nano Dimens.*, 2015, **6**:157
- [11]. Ahmadi R., Jalali Sarvestani M.R. *Iran. Chem. Commun.*, 2019, **7**:344
- [12]. Farhang Rik B., Ranjineh khojasteha R., Ahmadi R., Karegar Razi M. *Iran. Chem. Commun.*, 2019, **7**:405
- [13]. Zohari N., Abrishami F., Ebrahimikia M. *Zaac*, 2016, **13**:749
- [14]. Ahmadi R., Pirahan Froush M. *Ann. Mil. Health. Sci. Res.*, 2014, **12**:9
- [15]. Ahmadi R., Mirkamali E.S. *J. Phys. Theor. Chem. IAU Iran.*, 2016, **13**:297
- [16]. Ahmadi R., Ebrahimikia M. *Phys. Chem. Res.*, 2017, **5**:617
- [17]. Shemshaki L., Ahmadi R. *Int. J. New. Chem.*, 2015, **2**:247
- [18]. Ahmadi R., Madahzadeh Darini N. *Int. J. Bio-Inorg. Hybr. Nanomater.*, 2016, **5**:273
- [19]. Ahmadi R., Shemshaki L. *Int. J. Bio-Inorg. Hybr. Nanomater.*, 2016, **5**:141
- [20]. Ahmadi R., Jalali Sarvestani M.R. *Phys. Chem. Res.*, 2018, **6**:639
- [21]. Jalali Sarvestani M.R., Ahmadi R. *Int. J. New. Chem.*, 2018, **5**:409
- [22]. Jalali Sarvestani M.R., Ahmadi R. *Int. J. New. Chem.*, 2017, **4**:400
- [23]. Ahmadi R., Jalali Sarvestani M.R. *Int. J. Bio-Inorg. Hybrid. Nanomater.*, 2017, **6**:239
- [24]. Ahmadi R. *Int. J. Nano. Dimens.*, 2107, **8**:250
- [25]. Culebras M., Lopez A.M., Gomez C.M., Cantarero A. *Sens. Actuators. A. Phys.*, 2016, **239**:161
- [26]. [Mikkelsen S. R. Cortón E. Bioanalytical Chemistry. Wiley-Interscience: Michigan 2004; p 145](#)
- [27]. Ravi P., Gore M.G., Tewari S.P., Sikder A.K. *Mol. Simul.*, 2013, **38**:218
- [28]. Jalali Sarvestani M.R., Ahmadi R. *Int. J. New. Chem.*, 2017, **4**:400
- [29]. Jalali Sarvestani M.R., Ahmadi R. *J. Water. Environ. Nanotechnol.*, 2019, **4**:48
- [30]. Jalali Sarvestani M.R., Ahmadi R. *J. Phys. Theor. Chem.*, 2018, **15**:15
- [31]. Sharifi A., Hajiaghababaei L., Suzangarzadeh S., Jalali Sarvestani M.R. *Anal. Bioanal. Electroch.*, 2017, **9**:888

- [32]. Jalali Sarvestani M.R., Hajiaghababaei L., Najafpour J., Suzangarzadeh S. *Anal. Bioanal. Electroch.*, 2018, **10**:675
- [33]. Frisch M.J., Trucks G.W., Schlegel H.B., Scuseria G.E., Robb M.A., Cheeseman J.R., Scalman G., Barone V., Mennucci B., Petersson G.A., Nakatsuji H., Caricato M., Li X., Hratchian H.P., Izmaylov A.F., Bloino J., Zheng G., Sonnenberg J.L., Hada M., Ehara M., Toyota K., Fukuda R., Hasegawa J., Ishida M., T. Nakajima, Honda Y., Kitao O., Nakai H., Vreven T., Montgomery J.A., Jr., Peralta J.E., Ogliaro F., Bearpark M., Heyd J.J., Brothers E., Kudin K.N., Staroverov V.N., Kobayashi R., Normand J., Raghavachari K., Rendell A., Burant J.C., Iyengar S.S., Tomasi J., Cossi M., Rega N., Millam J.M., Klene M., Knox J.E., Cross J.B., Bakken V., Adamo C., Jaramillo J., Gomperts R., Stratmann R.E., Yazyev O., Austin A.J., Cammi R., Pomelli C., Ochterski J.W., Martin R.L., Morokuma K., Zakrzewski V.G., Voth G.A., Salvador P., Dannenberg J.J., Dapprich S., Daniels A.D., Farkas O., Foresman J.B., Ortiz J.V., Cioslowski J., Fox D.J. *Gaussian 09*. Revision A.02 ed.; Gaussian, Inc.: Wallingford CT, 2009
- [34]. Becke A.D. *J. Chem. Phys.*, 1993, **98**:5648
- [35]. Becke A.D. *Phys. Rev. A*, 1998, **38**:3098
- [36]. Lee C., Yang W., Parr R.G. *Phys. Rev. B*, 1988, **37**:785

How to cite this manuscript: Mohammad Reza Jalali Sarvestani, Roya Ahmadi*. A comprehensive DFT study on the adsorption of tetryl on the surface of graphene. *Asian Journal of Green Chemistry*, 4(3) 2020, 269-282. DOI: 10.22034/AJGC/2020.3.4